Available online at www.sciencedirect.com
ScienceDirect
International Journal of Pharmaceutics 340 (2007) 134–142
INTERNATIONAL JOURNAL OF PHARMACEUTICS
www.elsevier.com/locate/ijpharm

Pharmaceutical Nanotechnology

Chitosan/cyclodextrin nanoparticles as macromolecular drug delivery system

Alexander H. Krauland, María José Alonso *

Department of Pharmaceutical Technology, Faculty of Pharmacy, University of Santiago de Compostela, Spain

Received 17 November 2006; received in revised form 2 March 2007; accepted 6 March 2007
Available online 12 March 2007

Abstract

The aim of this study was to generate a new type of nanoparticles made of chitosan (CS) and carboxymethyl-β-cyclodextrin (CM-β-CD) and to evaluate their potential for the association and delivery of macromolecular drugs. CS and CM-β-CD or mixtures of CM-β-CD/tripolyphosphate (TPP) were processed to nanoparticles via the ionotropic gelation technique. The resulting nanoparticles were in the size range of 231–383 nm and showed a positive zeta potential ranging from +20.6 to +39.7 mV. These nanoparticles were stable in simulated intestinal fluid pH 6.8 at 37 °C for at least 4 h. Elemental analysis studies revealed the actual integration of CM-β-CD to CS nanoparticles. Insulin and heparin used as macromolecular model drugs, could be incorporated into the different nanocarriers with association efficiencies of 85.5–93.3 and 69.3–70.6%, respectively. The association of these compounds led to an increase of the size of the nanoparticles (366–613 nm), with no significant modification of their zeta potentials (+23.3 to +37.1 mV). The release profiles of the associated macromolecules were highly dependent on the type of molecule and its interaction with the nanomatrix: insulin was very fast released (84–97% insulin within 15 min) whereas heparin remained highly associated to the nanoparticles for several hours (8.3–9.1% heparin within 8 h). In summary, CS-CD (cyclodextrin) nanoparticles may be considered as nanocarriers for the fast or slow delivery of macromolecules.

Keywords: Nanoparticles; Chitosan; Cyclodextrins; Insulin; Heparin

1. Introduction

Important efforts and advances in biotechnology have facilitated the production of macromolecules like polypeptides, proteins and polysaccharides. As parenteral administration of macromolecular drugs can cause pain, stress by multiple injections and possible infections, non-invasive forms of macromolecular drug application would be highly appreciated. Alternative ways of drug administration like oral or nasal application would present a more convenient application form and would increase patient compliance dramatically. Unfortunately, most macromolecular drugs show very low bioavailabilities when administered via these alternative ways mentioned above (Illum, 1996). This low bioavailability is the result of different barriers, namely the enzymatic barrier, the absorption barrier and in the case of nasal administration the mucociliary clearance. A possibility to overcome these barriers is the use of nanocarriers, that are able to cross and transport associated molecules through the mucosal barrier, thereby also preventing the enzymatic attack. The size of these nanocarriers is an important factor for passing mucosae (Jani et al., 1990; Desai et al., 1997). Another critical parameter for the efficacy of nanosized drug delivery systems is the character of their surface. The use of mucoadhesive and absorption enhancing polymers for nanocarrier generation could still improve their efficacy. CS has shown in different studies to prolong the residence time of drug delivery systems at the site of drug absorption (Soane et al., 1999) and is known to open transiently the tight junctions (Illum, 1998). Nanoparticles based on CS loaded with insulin displayed after nasal administration to rabbits a significant improved decrease of the blood glucose level compared to insulin applied in a CS solution (Fernández-Urrusuno et al., 1999a,b). Additionally, calcitonin coated CS nanocapsules led to a significant stronger hypocalcemic effect than a nanoemulsion administered orally to

* Corresponding author at: Department of Pharmacy and Pharmaceutical Technology, Faculty of Pharmacy, University of Santiago de Compostela, 15782 Santiago de Compostela, Spain. Tel.: +34 981 563100x14885; fax: +34 981 547148.
E-mail address: ffmjalon@usc.es (M.J. Alonso).

0378-5173/$ – see front matter © 2007 Elsevier B.V. All rights reserved.
doi:10.1016/j.ijpharm.2007.03.005

rats (Prego et al., 2005). Furthermore, CS nanoparticles and CS-coated nanoparticles have been shown to deliver tetanus toxoid to the immune system, thereby leading to humoral and mucosal immune responses (Vila et al., 2004).

Besides the use of polymeric nanocarriers as drug delivery systems, the above mentioned barriers could also be overcome via addition of cyclodextrins (CDs). CDs are cyclic oligosaccharides composed of α-(1 → 4)-linked α-D-glucosyl units (Aachmann et al., 2003). They possess a central hydrophobic cavity, whereas the outside of the torus is hydrophilic. With the internal hydrophobic surface of the cavity CDs are able to form inclusion complexes with drugs of adequate size. Macromolecular drugs representing too large molecules for total inclusion can partially be complexed by CDs via their hydrophobic side chains (Irie and Uekama, 1999). Aachmann et al. (2003) and Lovatt et al. (1996) characterised these possible complexation sites for insulin monomers. Also if only partially included into the CD cavity the stability of macromolecular drugs can significantly be improved (Dotsikas and Loukas, 2002). Additionally, CDs are known to enhance the solubility of the incorporated drug (Filipović-Grčić et al., 2000), to act as permeation enhancers for different macromolecular drugs (Merkus et al., 1991; Sakr, 1996; Yang et al., 2004) and to inhibit the activity of certain proteases (Matsubara et al., 1997).

Taking this information into account, the aim of this study was to combine the virtues of CS nanocarriers and of CDs in one drug delivery system intended for the delivery of macromolecules. We have recently developed nanoparticles made of CS and HPCDs (hydroxypropylcyclodextrins) and evaluated their ability to entrap hydrophobic drugs (Maestrelli et al., 2006). In this work, our idea was to obtain nanoparticles consisting of CS and the anionic CD CM-β-CD and to study the possibility to associate macromolecules. This anionic CD was chosen because it was expected to favourably interact with the cationic molecules of CS. Additionally, CM-β-CD has been shown to increase the stability of proteins comparably to other CD species (Sigurjónsdóttir et al., 1999). CS-CM-β-CD nanoparticles were therefore prepared via the ionotropic gelation method incorporating varying amounts of CM-β-CD. The resulting nanoparticles were characterised regarding their size, zeta potential, shape and process yield. Additionally, their composition was determined. Subsequently, nanoparticles were loaded with two macromolecular model drugs, with insulin and heparin. Size, zeta potential, shape, process yield, stability and drug release of resulting particles were determined in vitro.

2. Materials and methods

2.1. Materials

CS in the form of the hydrochloride salt (UP CL 113, batch FP-110-02) was purchased from Pronova Biopolymer AS (Oslo, Norway). Its degree of acetylation was certificated to be 14%. Pentasodium tripolyphosphate (TPP), insulin (from bovine pancreas), heparin sodium salt and trifluoroacetic acid (HPLC grade) were supplied by Sigma Chemical Co. (St. Louis, MO, USA). Na-carboxymethyl-β-cyclodextrin (CM-β-CD, molecular weight 1375) having a substitution degree of 3.00–3.50 was purchased from Fluka GmbH (Buchs, Switzerland), acetonitrile of HPLC grade was purchased from J.T. Baker (Phillipsburg, NJ, USA). Ultrapure water (MilliQ Plus, Millipore Iberica, Madrid, Spain) was used throughout.

2.2. Preparation of nanoparticles

CS/CM-β-CD and CS/CM-β-CD/TPP nanoparticles were prepared according to the procedure previously developed by our group (Calvo et al., 1997). Nanoparticles were spontaneously obtained via ionotropic gelation between the positively charged amino groups of CS and the negatively charged CM-β-CD and/or the negatively charged TPP. Briefly, 1 mL of an aqueous solution of CM-β-CD (3–10.5 mg/mL) or 1 mL of a mixture of the aqueous solutions of TPP (0.375–1.125 mg/mL) and CM-β-CD (0.75–10.5 mg/mL) were added to 3 mL of a CS solution (0.2%, w/v, pH 4.9) under magnetic stirring at room temperature. Magnetic stirring was maintained for 10 min to allow the complete stabilisation of the system. The nanoparticles were isolated by centrifugation in a glycerol bed (16,000 × *g*, 30 min, 25 °C) and then resuspended in 100 μL of ultrapure water by shaking using a vortrex. Control nanoparticles consisting of CS and TPP were prepared in the same way. Glycerol was used for centrifugation to enhance the resuspensability of centrifuged nanoparticles.

The chemical structures of CS, TPP and CM-β-CD are presented in Fig. 1. A schematic presentation of the structures of CS/TPP, CS/CM-β-CD/TPP and CS/CM-β-CD nanoparticles is given in Fig. 2.

For the association of insulin or heparin to the different nanoparticle systems, insulin or heparin was dissolved in the CM-β-CD/TPP or TPP phase in a concentration of 2.4 mg/mL. For nanoparticle systems lacking TPP, insulin was dissolved in 0.01N NaOH (5 mg/mL), and 0.48 mL of the insulin solution was added to the CM-β-CD phase to obtain also a final insulin concentration of 2.4 mg/mL. Nanoparticles were prepared as described above and resulting nanoparticles were isolated by centrifugation in a glycerol bed (16,000 × *g*, 30 min, room temperature). Supernatants were collected for determination of the amount of unbound insulin and heparin. Nanoparticles were then resuspended in 100 μL of ultrapure water.

The production yield of the nanoparticles was obtained by centrifuging fixed volumes of the nanoparticle suspensions (16,000 × *g*, 40 min, room temperature) without glycerol bed. The supernatants were discarded and the centrifugates were kept at 50 °C until constant weight. The production yield was calculated comparing the actual weight with the theoretical weight of the nanoparticles.

2.3. Physicochemical characterisation of nanoparticles

The size and zeta potential of the colloidal systems were determined by photon correlation spectroscopy and laser Doppler anemometry using a Zetasizer 3000 HS (Malvern Instruments, Malvern, United Kingdom). Each batch was analysed in triplicate.

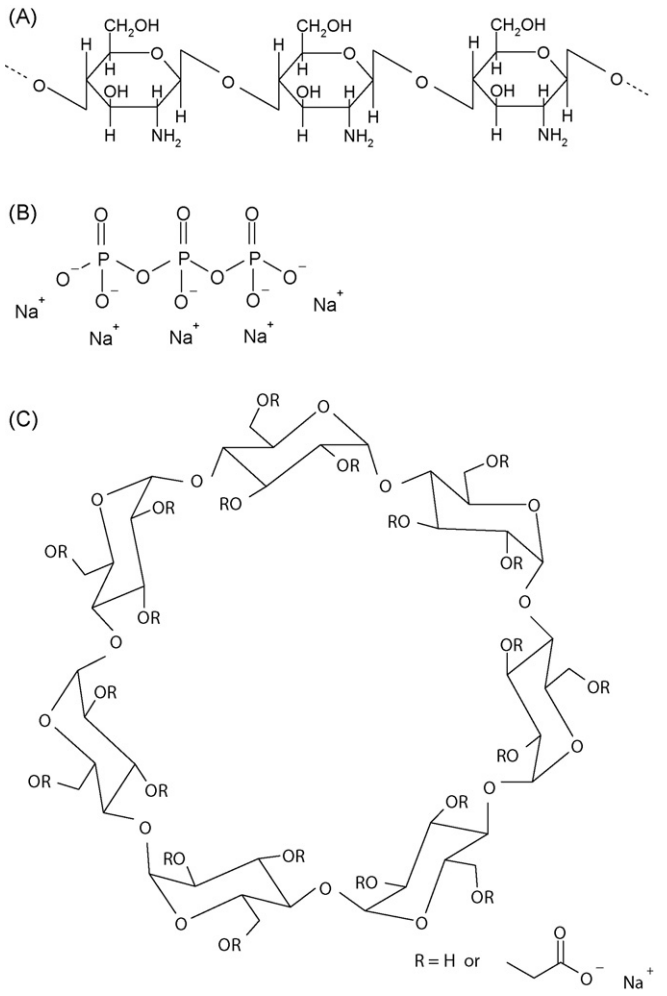

Fig. 1. The chemical structures of chitosan (A), pentasodium tripolyphosphate (B) and sodium carboxymethyl-β-cyclodextrin (C). R can be H or a sodium carboxymethyl group depending on the substitution degree.

The morphological examination of the nanoparticles was performed by transmission electron microscopy (TEM) (CM12 Philips, Eindhoven, The Netherlands). The samples were stained with 2% (w/v) phosphotungstic acid for 10 min, immobilised on copper grids with Formvar® and dried overnight for viewing by TEM.

2.4. Elemental analysis of nanoparticles

For elemental analysis unloaded nanoparticles were prepared as described above, but omitting glycerol during centrifugation, and finally lyophilised (Telstar Cryodos, Terrassa, Spain). Samples of pure CS, pure CM-β-CD and lyophilised nanoparticles were analysed by Elemental Analyzer Fisons (model EA 1108, Thermo Finnigan, Italy) for their content of carbon (C), hydrogen (H) and nitrogen (N). The CS content of the sample was analysed by the amount of N content of the sample in comparison with that of pure CS. For CM-β-CD content determination, the C content arising from CS was calculated and subtracted from total C amount. This remaining amount of C was used for CM-β-CD quantification comparing that C amount with that of pure CM-β-CD. The remaining fraction of the nanoparticles composition was attributed to TPP.

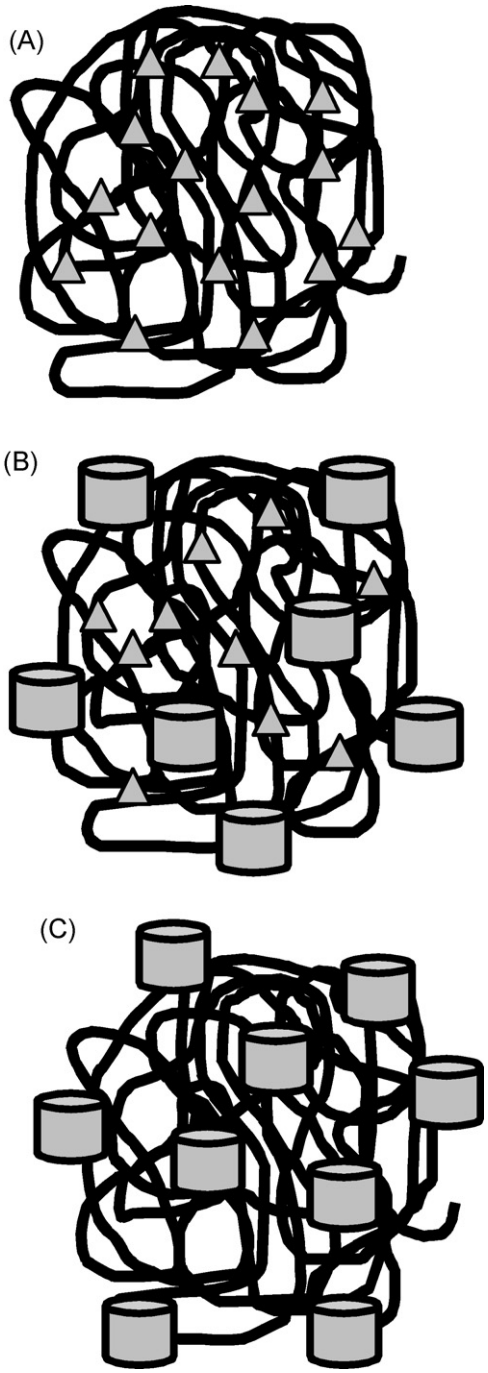

Fig. 2. Schematic presentation of the structures of CS/TPP (A), CS/CM-β-CD/TPP (B) and CS/CM-β-CD (C) nanoparticles, (▬) CS, (△) TPP and (⬭) CM-β-CD.

2.5. Loading and association efficiency of nanoparticles

The association efficiencies of the nanoparticle preparations were determined after isolation of nanoparticles by centrifugation as described in Section 2.2. The amount of unbound insulin was determined in the supernatant by HPLC analyses (Agilent

1100 Series, Santa Clara, CA, USA). A method described by Marschütz and Bernkop-Schnürch (2000) was thereby modified. Briefly, 20 μL of the supernatant was injected into HPLC. Insulin and/or degradation products were separated on a protein and peptide C18 column (Grace Vydac, W.R. Grace & Co., Columbia, MD, USA) at room temperature. Gradient elution was performed as follows: flow rate 1.0 mL/min, 0–10 min; linear gradient from 70% A/30% B to 39% A/61% B (eluent A: 0.1% trifluoroacetic acid in water; eluent B: acetonitrile). Insulin and/or degradation products were detected by absorbance at 220 nm with a diode array absorbance detector. Concentrations of insulin were quantified from integrated peak areas and calculated by interpolation from an according standard curve.

The amount of unbound heparin in the supernatant was determined using a colorimetric method (Stachrom® Heparin, Diagnostica Stago, Asnieres, France).

The loading efficiency and the association efficiency of insulin and heparin, respectively, were calculated as presented below:

$$\text{Loading efficiency} = \frac{\text{Total amount of drug} - \text{Amout of unbound drug}}{\text{Nanoparticles weight}} \times 100$$

$$\text{Association efficiency} = \frac{\text{Total amount of drug} - \text{Amout of unbound drug}}{\text{Total amount of drug}} \times 100$$

2.6. Stability study in intestinal medium

Selected nanoparticle formulations were prepared and centrifugated in presence of glycerol. Nanoparticles and insulin-loaded nanoparticles were tested for their stability in intestinal medium taking into account the change of the size of nanoparticles and possible precipitations. Nanoparticles were incubated in simulated intestinal fluid pH 6.8 at 37 °C (USP XXVI, without pancreatin) with agitation of 100 rpm. Samples were collected for insulin loaded nanoparticles after 30, 60 and 120 min and for non-loaded particles additionally after 240 min and the size distribution of the nanoparticles was measured by photon correlation spectroscopy. Size of the nanoparticles at different time points was referred to their size measured in water.

2.7. In vitro release studies

Insulin release studies were performed by incubating 0.1 mg insulin-loaded nanoparticles in 1 mL of simulated intestinal fluid (SIF), pH 6.8, at 37 °C. Heparin release studies were carried out by incubating 0.1 mg heparin-loaded nanoparticles in 1 mL of ultrapure water. At appropriate intervals, the samples were filtered and the amount of released insulin was evaluated by HPLC analysis and the amount of released heparin by the heparin kit described above. Concentrations of insulin and heparin were quantified and calculated by interpolation from an according standard curve.

3. Results and discussion

3.1. Preparation and characterisation of nanoparticles

Nanoparticles of CS and TPP and/or CM-β-CD were prepared via the ionotropic gelation technique. This method utilises the ionic interaction between the positively charged CS and the negatively charged TPP, and the ability of CS to form a gel after contact with polyanions by forming inter- and intramolecular linkages (Calvo et al., 1997). The ionic gelation process is extremely mild and involves the mixture of two aqueous phases at room temperature. In the present study the negatively charged CD CM-β-CD could also be incorporated into CS/TPP nanoparticles.

In previous studies we have observed that the amount of HP-β-CD that could be associated to CS nanoparticles was limited by the neutral nature of the CD (not published). Therefore, in this study we decided to add a negatively charged CD derivative, which should be incorporated more effectively into nanoparticles because of stronger ionic interactions with the positively charged CS. CM-β-CD, which is generally used for chiral separation of drugs (Lecnik et al., 2001; Perrin et al., 2006), but that also has shown to stabilise the protein salmon calcitonin at pH 6 (Matsubara et al., 1997), was chosen for this study.

Not only the introduction of CM-β-CD to CS/TPP led to nanoparticles, also nanoparticles could have been prepared in the absence of the polyanion TPP, only by mixing CS with different amounts of CM-β-CD. Resulting particles showed a comparable size as CS/CM-β-CD/TPP nanoparticles and reference particles of CS/TPP. All particles were in the nano-sized range and exhibited a positive zeta potential. The phase diagram (Fig. 3) reveals that only for specific ratios of CM-β-CD and TPP or in the case of CS/CM-β-CD nanoparticles for specific CM-β-CD concentrations nanoparticle formation could take place. If the initial total amount of CM-β-CD/TPP or the initial amount of CM-β-CD was too low, no nanoparticles were formed or the quantity of the formed nanoparticles was too low for their char-

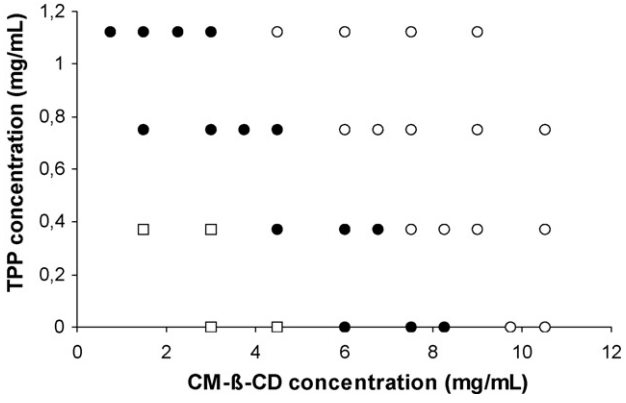

Fig. 3. Phase diagram of nanoparticle formation for CS/CM-β-CD/TPP and CS/CM-β-CD nanoparticles. CM-β-CD/TPP concentrations or CM-β-CD concentrations leading to formation of nanoparticles (●). Not adequate ratios led to formation of nanoparticles in a quantity too low for characterisation or no formation of nanoparticles (□) or precipitation or resuspension problems of nanoparticles (○), respectively.

Table 1
Physicochemical properties of selected CS nanoparticles prepared by addition of different ratios of CM-β-CD/TPP to a 0.2% CS solution (means ± S.D., $n = 3$)

Ratio CS/CM-β-CD/TPP	Size (nm)	PDI	Zeta potential (mV)	Yield (%)
4/5.5/0	231 ± 30	0.04–0.26	+20.6 ± 1.5	20.6 ± 5.3
4/5.5/0.25	Not resuspendable	–	–	–
4/4.5/0.25	272 ± 21	0.17–0.21	+21.3 ± 2.5	28.7 ± 3.5
4/4.5/0.5	Not resuspendable	–	–	–
4/3/0.5	328 ± 7	0.12–0.22	+26.6 ± 1.3	29.2 ± 1.8
4/3/0.75	Precipitation	–	–	–
4/1.5/0.75	383 ± 19	0.23–0.24	+36.3 ± 1.2	34.2 ± 1.4
4/1.5/1	Precipitation	–	–	–
4/0/1	287 ± 19	0.14–0.24	+39.7 ± 0.5	45.0 ± 2.7

acterisation. If the initial CM-β-CD/TPP amount or the initial amount of CM-β-CD was too high, precipitation occurred or the nanoparticles were not anymore resuspendable after their isolation.

Table 1 shows the size, polydispersity indices, zeta potentials and production yields of resulting CS/CM-β-CD, CS/CM-β-CD/TPP and control nanoparticles. In general, it was noted that the size, zeta potential and process yield of CM-β-CD-containing nanoparticles increased as the CM-β-CD/TPP ratios decreased. The lower zeta potential with increasing CM-β-CD amounts might be caused by an increased masking of free positively charged amino groups of CS. On the other hand, it could also be noted that the production yield increased when TPP was incorporated in the formulation.

The TEM photographs presented in Fig. 4a and b indicate that CS/CM-β-CD/TPP nanoparticles as well as CS/CM-β-CD nanoparticles had a spherical shape. These results agree well with the photographs of CS/TPP nanoparticles, which displayed a round, solid and consistent structure (Calvo et al., 1997).

3.2. Analysis of the composition of the nanoparticles

Elemental analysis of unloaded nanoparticles was performed to determine the composition of the different nanoparticle systems. After determination of the N and C content of the nanoparticles and after substraction of the C content of CS, the resulting amount of CM-β-CD could be calculated with the residual amount of C comparing it with the C content of pure CM-β-CD. As presented in Fig. 5, CM-β-CD could be very efficiently entrapped into the nanoparticles, representing more than 50% of the total components of the nanoparticles. The possibility of forming nanoparticles containing more than 50% of their weight of CM-β-CD is very important because of the low toxicity of the CD and also due to the special features of CD in terms of enhancing permeability (Irie and Uekama, 1999) and protecting drug molecules (Irie and Uekama, 1999). This high interaction between the CD and CS is justified by the presence of negatively charged carboxyl groups in the CD and their ionic interaction with the positively charged CS molecules.

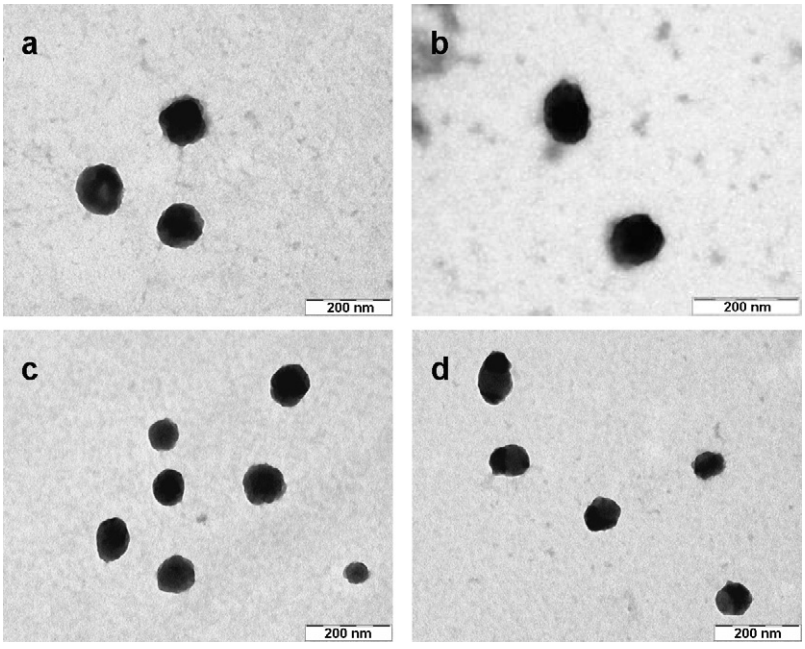

Fig. 4. Electron transmission micrographs of nanoparticles with CS/CM-β-CD/TPP ratios of 4/5.5/0 (a), 4/4.5/0.25 (b) and insulin loaded nanoparticles with CS/CM-β-CD/TPP ratios of 4/3/0 (c) and 4/4/0.25 (d).

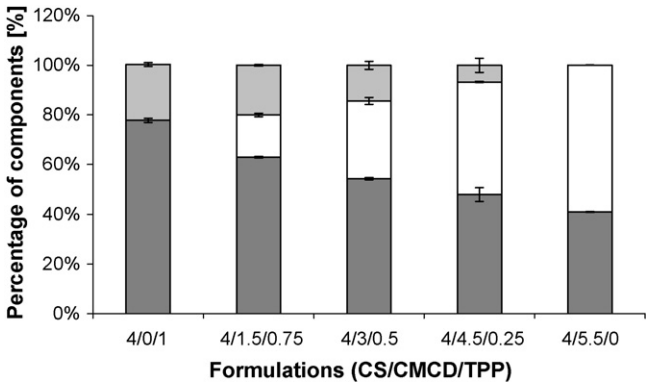

Fig. 5. Elemental analysis data of nanoparticles: (■) CS, (□) CM-β-CD and (▨) TPP (means ± S.D., $n = 3$).

3.3. Insulin association to nanoparticles

We chose insulin as a model polypeptide drug, as CDs are known to exhibit an additional favourable property especially in contact with insulin. Via perturbation of the hydrophobic contact between insulin monomers, CDs are believed to prevent self association of insulin monomers (Tokihiro et al., 1997) or favour the dissociation of insulin hexamers to dimers and further the dissociation of dimers to monomers as shown by circular dichroism studies (Shao et al., 1992). As monomers display a six-fold lower molecular weight over the hexameric form, they should permeate biomembranes more rapidly.

With respect to the characteristics of insulin-loaded nanoparticles, it should be noted that, due to the important interaction of insulin with CS, in some formulations the amount of CD had to be reduced in order to obtain nanoparticles with adequate redispersability during the isolation step. More specifically the CS/CM-β-CD/TPP ratios went from 4/5.5/0 and 4/4.5/0.25 to ratios of 4/3.5/0 and 4/4/0.25, respectively (Table 2a). The difficulties for resuspending the nanoparticles containing high amounts of both, insulin and CD, could be related to the negative charge of both molecules and the excessive reduction of the inherent positive charge of CS nanoparticles.

Table 2a shows that insulin-loaded CS/CM-β-CD and CS/CM-β-CD/TPP nanoparticles displayed a size in the range of 377–613 nm and a positive zeta potential (from +23 to +37 mV). As expected, insulin-loaded nanoparticles showed a lower zeta potential than the same unloaded formulations indicating the neutralization of the positive charge of CS by the negative charge of insulin.

Insulin could be incorporated very efficiently to all nanoparticle formulations, reaching association efficiencies of more than 85% (Table 2b). Increasing the amount of TPP and decreasing that of CM-β-CD it was possible to enhance the insulin association. Additionally, the pH of the insulin solution also plays an important role in the association process. In fact, insulin (p*I* 5.3) dissolved in 0.01N NaOH or in the CM-β-CD/TPP phase is negatively charged and the interaction between the protein and the positively charged CS is favoured, reaching an association efficiency of more than 85%. As described in another study positively charged insulin dissolved in 0.01N HCl, in contrast, could only be associated to CS/TPP nanoparticles in a 30.4% (Fernández-Urrusuno et al., 1999a,b). The association efficiencies of the present study agree well with the insulin association reported earlier in our research group for CS nanoparticles (Fernández-Urrusuno et al., 1999a,b). Also Boonsongrit et al. (2006) described entrapment of more than 90% of insulin to CS/TPP microparticles via ionotropic gelation in a pH area of 5.8–6.9 comparable to that in the present study.

With respect to the final loading efficiency of the nanoparticles, the formulation without TPP (4/3.5/0) was characterised by the highest loading efficiency with 68.4 ± 0.5% (Table 2b). In other words, these nanoparticles were composed of 68.4% of insulin and therefore only of 31.6% of CS/CM-β-CD. This is, from our knowledge, the greatest insulin loading efficiency of nanoparticles described so far in the literature.

Table 2a
Characteristics of selected insulin loaded CS/CM-β-CD, CS/CM-β-CD/TPP and CS/TPP nanoparticles

Ratio CS/CM-β-CD/TPP	Size (nm)	Polydispersity index	Zeta potential (mV)
4/3.5/0	377 ± 21	0.04–0.19	+26.2 ± 0.6
4/4/0.25	436 ± 34	0.10–0.23	+23.3 ± 0.4
4/3/0.5	555 ± 119	0.02–0.52	+26.0 ± 1.3
4/1.5/0.75	613 ± 124	0.11–0.58	+31.0 ± 1.5
4/0/1	454 ± 120	0.22–0.31	+37.1 ± 1.3

Concentration of insulin in CM-β-CD, CM-β-CD/TPP or TPP phase: 2.4 mg/mL (means ± S.D., $n = 3$).

Table 2b
Loading characteristics of insulin loaded CS/CM-β-CD, CS/CM-β-CD/TPP and CS/TPP nanoparticles

Ratio CS/CM-β-CD/TPP	Loading efficiency (%)	Association efficiency (%)	Yield (%)
4/3.5/0	68.4 ± 0.5	85.5 ± 0.4	19.2 ± 0.6
4/4/0.25	46.7 ± 0.8	88.6 ± 0.8	27.6 ± 2.3
4/3/0.5	38.5 ± 0.4	92.6 ± 0.6	39.4 ± 2.0
4/1.5/0.75	38.7 ± 0.5	93.3 ± 0.7	46.0 ± 2.4
4/0/1	34.7 ± 0.3	91.4 ± 0.4	58.8 ± 0.8

Concentration of insulin in CM-β-CD, CM-β-CD/TPP or TPP phase: 2.4 mg/mL (means ± S.D., $n = 3$).

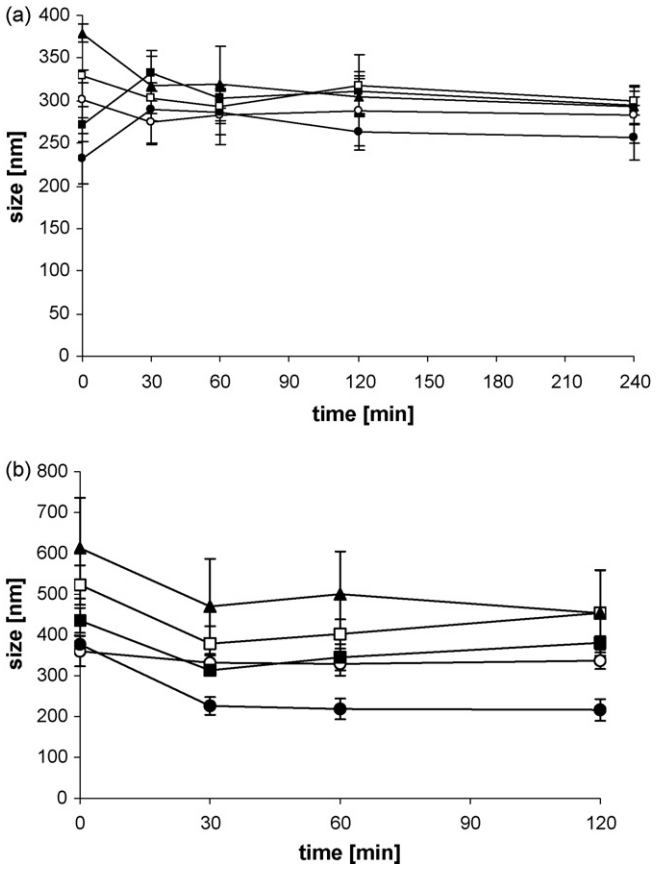

Fig. 6. (a) Stability of CS/CM-β-CD/TPP = 4/0/1 (◯), 4/1.5/0.75 (▲), 4/3/0.5 (□), 4/4.5/0.25 (■) and 4/5.5/0 (●) nanoparticles in simulated intestinal fluid, pH 6.8, 37 °C (means ± S.D., $n = 3$). (b) Stability of insulin loaded CS/CM-β-CD/TPP = 4/0/1 (◯), 4/1.5/0.75 (▲), 4/3/0.5 (□), 4/4/0.25 (■) and 4/3.5/0 (●) nanoparticles in simulated intestinal fluid, pH 6.8, 37 °C (means ± S.D., $n = 3$).

Finally, in Fig. 4c and d, it could be seen, that insulin-loaded CS/CM-β-CD/TPP and CS/CM-β-CD have a spherical shape, similar to that observed for unloaded nanoparticles.

3.4. Stability studies

Keeping in mind that the final application of these nanoparticles is their use for transmucosal delivery of macromolecules, we found it important to determine their stability in physiological conditions (pH 6.8 and 37 °C). The results showed that non-loaded nanoparticles did not suffer a significant change in their size following incubation for at least 4 h (Fig. 6a). However, it can be noted that upon contact with simulated intestinal fluid some formulations suffered a small size reduction, which could be related to the detachment of some of the components of the nanoparticles, whereas other formulations exhibited a size increase which could be ascribed to a swelling effect.

Insulin-loaded CS/CM-β-CD/TPP nanoparticles showed a stability of more than 2 h (Fig. 6b). As in the case of some blank nanoparticulate formulations, the size of nanoparticles decreased within the first 30 min of the experiment. This size reduction could be related to the fast release of insulin from the nanoparticle matrix.

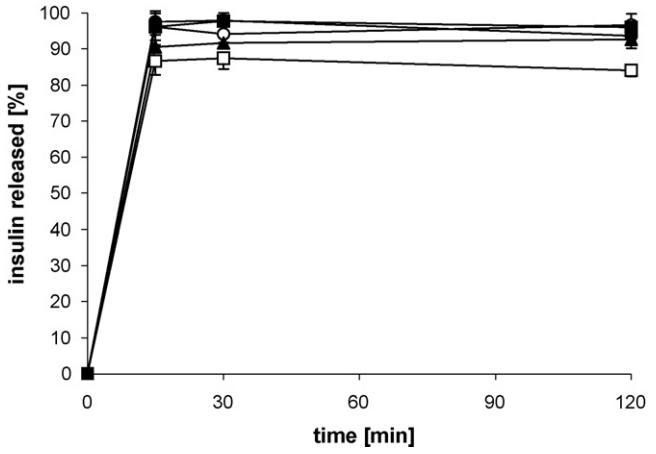

Fig. 7. Insulin release of insulin loaded CS/CM-β-CD/TPP = 4/0/1 (◯), 4/1.5/0.75 (▲), 4/3/0.5 (□), 4/4/0.25 (■) and 4/3.5/0 (●) nanoparticles in simulated intestinal fluid, pH 6.8, 37 °C (means ± S.D., $n = 3$).

3.5. In vitro release of insulin

As presented in Fig. 7, all different nanoparticle systems released 84–97% of incorporated insulin within 15 min. The varying composition of the nanoparticles regarding different amounts of TPP and CM-β-CD did not influence the release of insulin. This fast release agrees well with the results of other studies where almost the same amount of insulin was released from CS/TPP micro- or nanoparticles within the same time period (Boonsongrit et al., 2006). Only release studies of nanoparticles at pH 5.5 and 6.4, respectively, displayed more sustained release profiles (Fernández-Urrusuno et al., 1999a,b; Ma et al., 2002), which could be attributed to the pH of the release mediums near to the isoelectric point of insulin (5.3). The fast release of insulin from the nanoparticles could be understood as a consequence of its weak ionic interaction with CS (Boonsongrit et al., 2006) and its subsequent disassociation in physiological pH at high ionic strength. In addition, it has been shown that negatively charged drugs form only labile complexes with CM-β-CD (Hanna et al., 2004) due to the fact that ionic repulsions counteract the hydrophobic interactions.

These very fast releasing formulations could be of particular interest for improving the nasal absorption of insulin. Indeed, due to the lack of fluid in the nasal cavity it could be presumed that insulin would be released from the nanoparticles once they reach and interact with the nasal epithelium. Current in vivo studies have been designed to assert the efficacy of these formulations.

3.6. Heparin association and release from nanoparticles

As second macromolecular model drug heparin was chosen, a highly soluble glycosaminoglycan, used for its anticoagulant activity. Different cell studies revealed an increased permeability of heparin in the presence of CDs compared to heparin without permeation enhancers (Yang et al., 2004). Additionally, these heparin/CD combinations led to an increased bioavailability after nasal administration to rats (Yang et al., 2004). Therefore,

Table 3a
Characteristics of selected heparin loaded CS/CM-β-CD and CS/TPP nanoparticles

Ratio CS/CM-β-CD/TPP	Size (nm)	Polydispersity index	Zeta potential (mV)
4/0/0.25	366 ± 30	0.39–0.51	+35.5 ± 0.8
4/1/0.25	Not resuspendable	–	–
4/1/0	531 ± 10	0.35–0.41	+32.3 ± 0.6
4/1.5/0	574 ± 24	0.42–0.55	+28.8 ± 0.9
4/2/0	Not resuspendable	–	–

Concentration of heparin in CM-β-CD or TPP phase: 2.4 mg/mL (means ± S.D., $n = 3$).

a combination of heparin and CD within nanoparticles should be advantageous.

Heparin was added to the nanoparticles formation medium in the same amount as insulin. As heparin represents a much more negatively charged drug than insulin used above its isoelectric point, TPP or CM-β-CD amounts had to be reduced in order to achieve resuspendable nanoparticles (Table 3a). The resulting heparin-loaded CS nanoparticles of CM-β-CD or TPP displayed a size in the range of 366–574 nm and a positive zeta potential (from +28.8 to +35.5 mV). The association of heparin to the nanoparticles was high, however, in contrast to our expectations the association efficiency values (69.3–70.6%; Table 3b) were lower than those of insulin (85.5–93.3%). Indeed, heparin is a highly negatively charged molecule and, consequently, it was expected to interact with CS more efficiently than insulin. However, the reduced association, as compared to that of insulin, could be related to the necessity to reformulate the nanoparticles composition in order to obtain well-defined and resuspendable nanoparticles. Despite these differences, it should be kept in mind that the association of heparin was also very high reaching final loading efficiencies of 43.3–49.9%. This indicates that half of the weight of the nanoparticles is heparin.

In contrast to insulin release studies that were performed in SIF, heparin release studies had to be conducted in ultrapure water. Heparin loaded nanoparticles were not stable in SIF and precipitated in this medium. To guarantee the stability of nanoparticles during drug release we decided to perform heparin release in ultrapure water as a preliminary study. In this medium, in which heparin is well soluble, heparin loaded nanoparticles showed high stability. In future studies a reformulation is planned to achieve heparin loaded nanoparticles also stable in SIF.

With respect to the release of heparin from the nanoparticle systems, the results in Fig. 8 show that only 8.3–9.1% of heparin were released following incubation in ultrapure water for up to 8 h. Almost the same profile was observed for all formulations tested and no significant differences could be observed comparing the TPP system with the CM-β-CD systems. However,

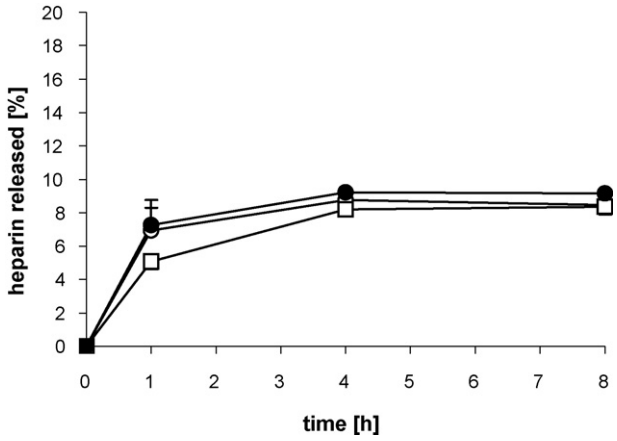

Fig. 8. Heparin release of heparin loaded CS/CM-β-CD/TPP = 4/0/0.25 (◯), 4/1.5/0 (□), 4/1/0 (●) nanoparticles in ultrapure water, 37 °C (means ± S.D., $n = 3$).

regarding only the two CM-β-CD containing nanoparticles, the 4/1/0 system showed a significantly ($p < 0.05$) higher release of heparin than the 4/1.5/0 system within the first hour, maybe because of steric hindrance of heparin by the higher amount of CM-β-CD in the 4/1.5/0 formulation. The slow heparin release of the three investigated nanoparticle systems could on the one hand be understood on the basis of a strong interaction between heparin and CS, mediated by the important high charges of both molecules. On the other hand, slow heparin release might additionally be based on the release medium ultrapure water. Heparin nanoparticles might show different release kinetics in SIF because of the presence of electrolytes. This will be evaluated in future studies upon reformulated, in SIF stable heparin nanoparticles. Nevertheless, this in vitro release experiment in ultrapure water can be seen as a first step of an in vitro characterisation of heparin loaded CS/CM-β-CD nanoparticles.

A slow release behaviour of the nanoparticles could be of interest for a potential application of the nanoparticles for oral administration. In fact, it would be desirable that the release process starts only once the nanoparticles reach and interact with

Table 3b
Loading characteristics of heparin loaded CS/CM-β-CD and CS/TPP nanoparticles

Ratio CS/CM-β-CD/TPP	Loading efficiency (%)	Association efficiency (%)	Yield (%)
4/0/0.25	43.3 ± 0.6	70.6 ± 0.9	44.6 ± 3.2
4/1/0	49.9 ± 0.4	69.3 ± 0.5	33.7 ± 1.3
4/1.5/0	43.7 ± 0.4	70.5 ± 0.7	36.3 ± 0.0

Concentration of heparin in CM-β-CD or TPP phase: 2.4 mg/mL (means ± S.D., $n = 3$).

the absorbing intestinal epithelium. While further in vitro studies have to be performed as mentioned above to confirm the usefulness of CS/CM-β-CD nanoparticles for oral delivery of heparin, it is worthwhile to mention that previously reported heparin-loaded nanoparticles made of positively charged Eudragits, also displayed a very slow in vitro release (about 2–11%) and led to very positive in vivo absorption results (Jiao et al., 2001, 2002).

4. Conclusion

We have designed a new nanoparticulate delivery carrier for macromolecules, which consists of the mucoadhesive polymer CS and a negatively charged CD, via the very mild ionotropic gelation technique. The final composition of the system (CS/CD ratio) can be modified by adjusting the formulation conditions. Moreover, the resulting nanoparticles exhibited a small size, a positive zeta potential and a great capacity for the association of two selected macromolecules: insulin and heparin. These results render the designed nanocarriers as possible candidates for improving the absorption of macromolecules following either oral or nasal administration.

Acknowledgement

This work was supported by the European Commission within the Sixth Framework Programme – NanoBiosaccharides – Contract number 013882.

References

Aachmann, F.L., Otzen, D.E., Larsen, K.L., Wimmer, R., 2003. Structural background of cyclodextrin–protein interactions. Protein Eng. 16, 905–912.

Boonsongrit, Y., Mitrevej, A., Mueller, B.W., 2006. Chitosan drug binding by ionic interaction. Eur. J. Pharm. Biopharm. 62, 267–274.

Calvo, P., Remuñan-Lopez, C., Vila-Jato, J.L., Alonso, M.J., 1997. Novel hydrophilic chitosan-polyethylene oxide nanoparticles as protein carriers. J. Appl. Pol. Sci. 63, 125–132.

Desai, M.P., Labhasetwar, V., Walter, E., Levy, R.J., Amidon, G.L., 1997. The mechanism of uptake of biodegradable microparticles in Caco-2 cells is size dependent. Pharm. Res. 14, 1568–1573.

Dotsikas, Y., Loukas, Y.L., 2002. Kinetic degradation study of insulin complexed with methyl-beta cyclodextrin. Conformation of complexation with electrospray mass spectroscopy and ^{1}H NMR. J. Pharm. Biomed. Anal. 29, 487–494.

Fernández-Urrusuno, R., Romani, D., Calvo, P., Vila-Jato, J.L., Alonso, M.J., 1999a. Development of a freeze-dried formulation of insulin-loaded chitosan nanoparticles intended for nasal administration. S. T. P. Pharm. Sci. 9, 429–436.

Fernández-Urrusuno, R., Calvo, P., Remuñan-Lopez, C., Vila-Jato, J.L., Alonso, M.J., 1999b. Enhancement of nasal absorption of insulin using chitosan nanoparticles. Pharm. Res. 16, 1576–1581.

Filipović-Grčić, J., Voinovich, D., Moneghini, M., Bećirević-Laćan, M., Magarotto, L., Jalšenjak, I., 2000. Chitosan microspheres with hydrocortisone and hydrocortisone-hydroxypropyl-β-cyclodextrin inclusion complex. Eur. J. Pharm. Sci. 9, 373–379.

Hanna, K., de Brauer, Ch., Germain, P., 2004. Cyclodextrin-enhanced solubilization of pentachlorophenol in water. J. Env. Manage. 71, 1–8.

Illum, L., 1996. Nasal delivery. The use of animal models to predict performance in man. J. Drug Target. 3, 427–442.

Illum, L., 1998. Chitosan and its use as a pharmaceutical excipient. Pharm. Res. 15, 1326–1331.

Irie, T., Uekama, K., 1999. Cyclodextrins in peptide and protein delivery. Adv. Drug Deliv. Rev. 36, 101–123.

Jani, P.U., Halbert, G.W., Landridge, J., Florence, A.T., 1990. Nanoparticle uptake by the rat gastrointestinal mucosa: quantitation and particle size dependency. J. Pharm. Pharmacol. 42, 821–826.

Jiao, Y.Y., Ubrich, N., Marchand-Arvier, M., Vigneron, C., Hoffman, M., Maincent, P., 2001. Preparation and in vitro evaluation of heparin-loaded polymeric nanoparticles. Drug Deliv. 8, 135–141.

Jiao, Y.Y., Ubrich, N., Marchand-Arvier, M., Vigneron, C., Hoffman, M., Lecompte, T., Maincent, P., 2002. In vitro and in vivo evaluation of oral heparin-loaded polymeric nanoparticles in rabbits. Circulation 105, 230–235.

Lecnik, O., Schmid, M.G., Kappe, C.O., Gubitz, G., 2001. Chiral separation of pharmacologically active dihydropyrimidones with carboxymethyl-beta-cyclodextrin. Electrophoresis 22, 3198–3202.

Lovatt, M., Cooper, A., Camilleri, P., 1996. Energetics of cyclodextrin-induced dissociation of insulin. Eur. Biophys. J. 24, 354–357.

Ma, Z., Yeoh, H.H., Lim, L.-Y., 2002. Formulation pH modulates the interaction of insulin with chitosan nanoparticles. J. Pharm. Sci. 91, 1396–1404.

Maestrelli, F., Garcia-Fuentes, M., Mura, P., Alonso, M.J., 2006. A new drug nanocarrier consisting of chitosan and hydroxypropylcyclodextrin. Eur. J. Pharm. Biopharm. 63, 79–86.

Marschütz, M.K., Bernkop-Schnürch, A., 2000. Oral peptide drug delivery: polymer-inhibitor conjugates protecting insulin from enzymatic degradation in vitro. Biomaterials 21, 1499–1507.

Matsubara, M., Ando, Y., Irie, T., Uekama, K., 1997. Protection afforded by maltosyl-β-cyclodextrin against α-chymotrypsin-catalyzed hydrolysis of a luteinizing hormone-releasing hormone agonist, buserelin acetate. Pharm. Res. 14, 1401–1405.

Merkus, F.W.H.M., Verhoef, J., Romeijn, S.G., Schipper, N.G.M., 1991. Absorption enhancing effect of cyclodextrins on intranasally administered insulin in rats. Pharm. Res. 8, 588–592.

Perrin, C., Coussot, G., Lefebrve, I., Perigaud, C., Fabre, H., 2006. Separation of 3′-azido-2′,3′-dideoxythymidine pronucleotide diastereoisomers in biological samples by CZE with cyclodextrin addition. J. Chromatogr. A 1111, 139–146.

Prego, C., García, M., Torres, D., Alonso, M.J., 2005. Transmucosal macromolecular drug delivery. J. Control. Rel. 101, 151–162.

Sakr, F.M., 1996. Nasal administration of glucagons combined with dimethyl-β-cyclodextrin: comparison of pharmacokinetics and pharmacodynamics of spray and powder formulations. Int. J. Pharm. 132, 189–194.

Shao, Z., Krishnamoorthy, R., Mitra, A.K., 1992. Cyclodextrins as nasal absorption promoters of insulin: mechanistic evaluations. Pharm. Res. 9, 1157–1163.

Sigurjónsdóttir, J.F., Loftsson, T., Másson, M., 1999. Influence of cyclodextrins on the stability of the peptide salmon calcitonin in aqueous solution. Int. J. Pharm. 186, 205–213.

Soane, R.J., Frier, M., Perkins, A.C., Jones, N.S., Davis, S.S., Illum, L., 1999. Evaluation of the clearance characteristics of bioadhesive systems in humans. Int. J. Pharm. 178, 55–65.

Tokihiro, K., Irie, T., Uekama, K., 1997. Varying effects of cyclodextrin derivatives on aggregation and thermal behavior of insulin in aqueous solution. Chem. Pharm. Bull. 45, 525–531.

Vila, A., Sánchez, A., Janes, K.A., Behrens, I., Kissel, T., Vila-Jato, J.L., Alonso, M.J., 2004. Low molecular weight chitosan nanoparticles as new carriers for nasal vaccine delivery to mice. Eur. J. Pharm. Biopharm. 57, 123–132.

Yang, T., Hussain, A., Paulson, J., Abbruscato, T.J., Ahsan, F., 2004. Cyclodextrins in nasal delivery of low-molecular-weight heparins: in vivo and in vitro studies. Pharm. Res. 21, 1127–1136.